

# Reversing the persistent current of particles in a driven optical ring lattice

L. Morales-Molina and E. Arévalo

*Instituto de Física, Facultad de Física, Pontificia Universidad Católica de Chile, Casilla 306, Santiago 22, Chile*

(Received 11 August 2015; published 27 October 2015)

We study the dynamics of persistent bosonic currents in closed-loop atom circuits in the form of ring lattices and under the action of time periodic driving. The closed-loop atom circuits are described by a Bose-Hubbard model in the presence of a Peierls phase and with periodic boundary conditions. We find that the motion of matter waves can be controlled with the help of an external driving only applied in one site of the ring lattice. For tuned values of the interaction strength between particles, we show that there exists a frequency range of the external driving where not only suppression but also reversion of the persistent bosonic currents is achieved. Applications of our results are discussed.

DOI: [10.1103/PhysRevA.92.043625](https://doi.org/10.1103/PhysRevA.92.043625)

PACS number(s): 03.75.Lm, 37.10.Jk, 05.60.Gg, 03.65.Vf

## I. INTRODUCTION

Optical rings have been proposed as an ideal experimental setting for testing the superfluid behavior in matter waves in closed-loop atom circuits [1]. In fact, persistent, closed-loop, bosonic currents of particles have been experimentally observed in optical rings upon breaking the time reversal symmetry [1,2]. In recent times, major experimental developments, mostly focus on the motion Bose-Einstein condensates over toroidal shape rings [3], have generated renewed interest [4] in the study of the motion of cold atoms in closed-loop atom circuits. These experiments have achieved building small optical rings [5], opening up a window for the exploration of atoms moving in small settings. For these systems, the Bose-Hubbard model has been shown to describe well the superfluid behavior of matter waves in ring lattices [1].

Since persistent currents or bosonic particles currently are experimentally feasible, controlling them has become an important issue of investigation to build future quantum devices [6,7]. In particular, the search for mechanisms to coherently control these persistent currents in closed-loop atom circuits, such as ring lattices, is a necessary step towards this goal.

An important property of boson particles of the same species is their interaction among each other. This property becomes relevant when two or more boson particles in an optical lattice share the same lattice site [8]. In the Bose-Hubbard model for bosons, this property is modeled as an on-site interaction. On the other hand, it is well known that, for integer fillings, the bosonic-interaction strength beyond some critical value can halt the motion of particles trapped in optical lattices [9]. Obviously, below this critical value the particles in the system can in principle move without restriction regardless of the occupation number. We show in what follows that the presence of an on-site interaction with a strength below the critical value can act in other ways to affect the motion of particles and/or currents in optical lattices.

In the context of ring lattices, a more complex scenario can be observed when the lattice is driven by ac fields [10]. In fact, the presence of ac fields offer two main advantages to the lattice system. First, it allows the construction of an artificial gauge field [11], where tunneling is assisted by ac fields, thus leading to the accumulation of the so-called Peierls phase [12]. Such a phase is needed when superfluid persistent currents of

particles are created in different ring-lattice configurations. Second, it can induce changes in the dynamics of interacting matter waves, including suppression of tunneling in a periodic lattice [13,14], tunneling of atoms in a double-well potential [15], ratchet dynamics [16], and others [17]. Yet, the full extent of ac-field applicability remains an open question.

In the present work we harness the on-site interaction to control the transport properties of persistent, closed-loop currents of particles in optical ring lattices. In particular, we show, by properly tuning the interaction strength [18], that it is possible to reverse a persistent current of particles in optical ring lattices in the presence of an on-site ac impurity.

In the context of superfluidity of matter waves in lattice rings, the presence of an on-site impurity can be interpreted as a barrier. The superfluid behavior of matter waves in the presence of a local stationary barrier has been explored in recent experiments [3] showing that a precise control of arresting the superfluid flow of particles can be achieved. In the present theoretical work, we go beyond the stationary barrier concept and study the effects arising from the interplay between a local ac barrier and the ubiquitous on-site interaction in optical ring lattices. In particular, we are concerned with frequency values of the ac barrier much higher than the characteristic frequencies of the system. In this high frequency regime, phenomena similar to dynamical localization [19] and/or coherent destruction of tunneling [20,21] can be expected to arise.

The present work is organized as follows. In Sec. II, we introduce the model for particles moving in a ring lattice in the presence of an ac driving applied on a single lattice site. In Sec. III, we study the dynamics for two particles on three lattice sites with the help of the energy spectrum as a function of both the amplitude of the ac driving and interaction strength between particles. In particular, we analytically show how, for two particles in three lattice sites, the bosonic current is reversed by tuning the amplitude of the driving. Numerical results for more particles in three, four, and six lattice sites are also considered and analyzed. In the last section, the results are summarized and applications are discussed.

## II. MODEL

The superfluid circulation of atoms in optical ring lattices have been studied by using the Bose-Hubbard model in the

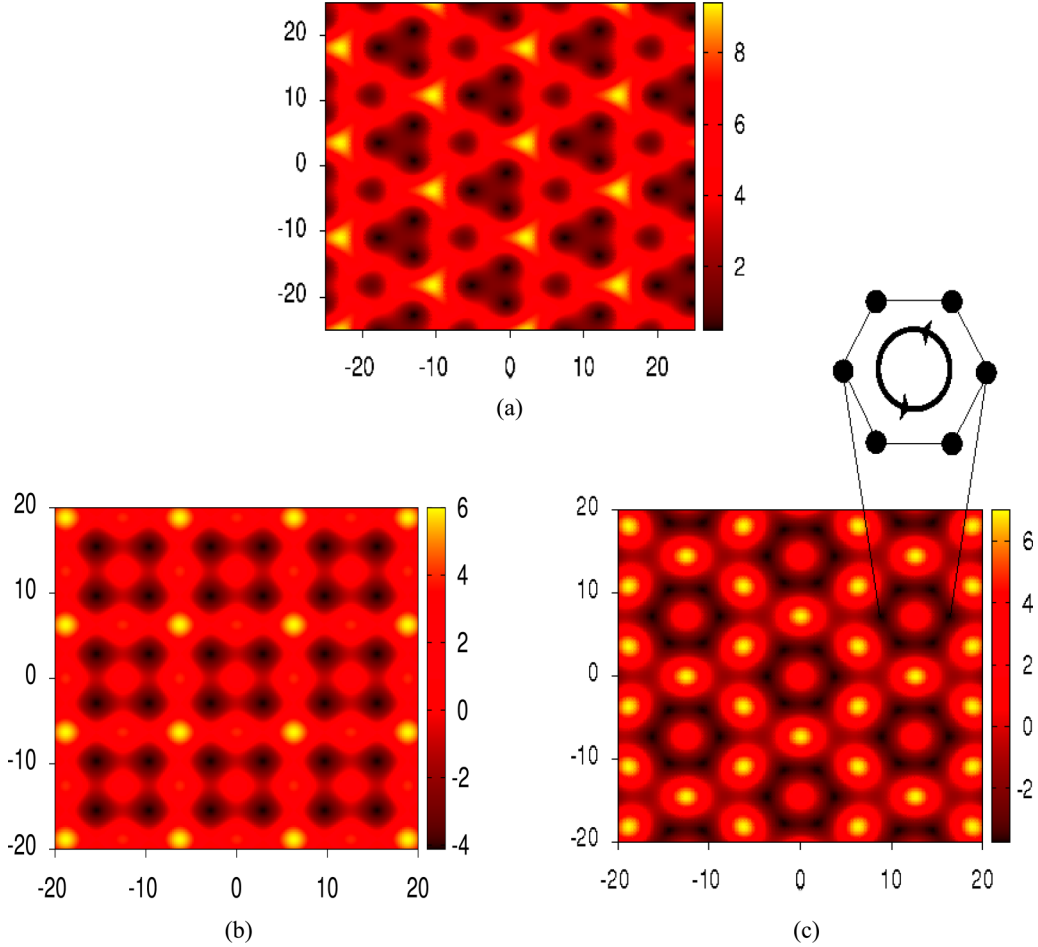


FIG. 1. (Color online) Optical potentials created by superimposing biharmonic lattices in directions forming angles of 90 degrees in (b) and 120 degrees in (a) and (c). (a) Array of triangular ring lattices. (b) Array of square ring lattices. (c) Array of hexagonal ring lattices. Dark regions correspond to the deep parts of the potential where the particles are usually trapped.

presence of a Peierls phase [1]. In the present analysis we also consider the additional presence of a single impurity that mimics an ac barrier in the ring lattice. In this case, the Bose-Hubbard Hamiltonian for the superfluid motion of bosons in optical ring lattices and in the presence of a time-dependent driving field reads as

$$\hat{H} = -\Omega \sum_i^L (e^{i\phi'} \hat{a}_i^\dagger \hat{a}_{i+1} + e^{-i\phi'} \hat{a}_{i+1}^\dagger \hat{a}_i) + \frac{U}{2} \sum_{i=1}^L \hat{n}_i (\hat{n}_i - 1) + \mathcal{A}(t) \sum_{i=1}^L \hat{a}_i^\dagger \hat{a}_i \delta_{i,i_0}, \quad (1)$$

where  $\hat{a}_i^\dagger$  ( $\hat{a}_i$ ), creates (annihilates) a particle at the  $i$ th site and  $\hat{n}_i = \hat{a}_i^\dagger \hat{a}_i$  is the particle number operator. In Eq. (1),  $\delta_{i,i_0}$  is the Kronecker delta with  $1 \leq i_0 \leq L$  and  $L$  is the total number of sites. Besides,  $\phi'$  in Eq. (1) is defined as  $\phi' = \phi/L$ , where  $\phi$  is the so-called Peierls phase. The Hamiltonian in Eq. (1) is written as the addition of three terms, which can be interpreted as follows. The first term of the Hamiltonian (1) is the kinetic term of the Hamiltonian whose strength is given by the hopping constant  $\Omega$ . The second term of the Hamiltonian (1) accounts for the on-site bosonic interaction with a strength

given by the constant  $U$ . The third term of the Hamiltonian (1) accounts for the impurity mimicking the barrier located at the  $i_0$  site of the ring lattice. This latter Hamiltonian term contains a coefficient  $\mathcal{A}(t)$ , which is in general time dependent and accounts for an external driving. In order to consider closed-loop particle currents in ring lattices the periodic boundary condition  $\hat{a}_{i+L}^\dagger = \hat{a}_i^\dagger$  must be satisfied.

Examples of the optical ring lattices that we are considering are shown in Fig. 1. These types of rings are currently being built by interference of several laser beams so that the intensity distribution is equivalent to a periodic superposition of two biharmonic optical potentials [22–24] on a two-dimensional plane (see also [25]).

#### A. Time independent system: stationary barrier

Let us first analyze the case when external driving does not depend on the time, i.e.,  $\mathcal{A}(t) = \text{constant}$ . So, in this case the barrier is stationary. A similar scenario has been discussed in the frame of superfluid persistent currents of bosonic particles in toroidal Bose-Einstein condensates, where the precise control in arresting superfluid flows has been achieved [3]. For few bosonic particles in a ring lattice, the

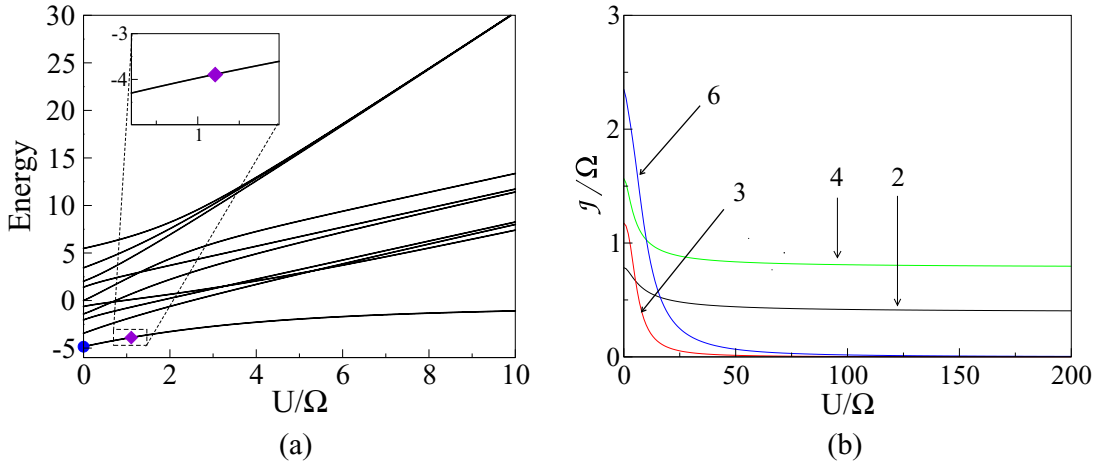


FIG. 2. (Color online) (a) Energy spectrum vs interaction strength  $U/\Omega$ .  $N = 3$ ,  $L = 3$ . The blue dot is the ground state for  $U/\Omega = 0$ , depicted in Fig. 3 for  $A/\omega = 0$ . The inset shows a section of energy values for the ground state where the symbol of a diamond depicts the energy state with  $U/\Omega = 1.105$ . This symbol is also depicted in the left panel, second row of Fig. 5 for  $A/\omega = 0$ . (b) Current of particles of the ground state vs interaction of particles for two, three, four, and six particles moving in a three-site ring ( $L = 3$ ).  $\phi' = \pi/5$ .

particle current operator  $\hat{J}$  is defined as

$$\hat{J} = -\frac{i\Omega}{L} \sum_i^L (e^{i\phi'} \hat{a}_i^\dagger \hat{a}_{i+1} - e^{-i\phi'} \hat{a}_{i+1}^\dagger \hat{a}_i). \quad (2)$$

By studying the behavior of these particle currents in ring lattices in the presence of a constant barrier, we observe that the magnitude of the currents in general decreases as the barrier height increases. In fact, the persistent closed-loop current of particles vanishes in the limiting case of an infinite barrier. Of course, this result is expected since an infinite barrier height, in practice, corresponds to a lattice with two separated extremes. So, no persistent closed-loop current of particles can exist. Notice that for Bose-Einstein condensates the precise control in arresting superfluid flows is associated with dissipative effects [3], because the presence of a barrier implies work against the persistent motion of particles.

In the particular case of the absence of interaction and external driving, i.e.,  $\mathcal{A}(t) = U = 0$ , Eq. (1) can only describe the ground state of a superfluid system [see the lowest energy state in Fig. 2(a)]. Notice that the ground state appears well separated from the rest of the energy states.

In the presence of the interaction ( $U \neq 0$ ), we observe that, in the regime where  $U/\Omega \gg 1$ , the particle current of the ground state [Fig. 2(b)] depends only on the filling number. In this latter regime, the current exhibits finite constant values if the filling number is noninteger; otherwise the current vanishes, as shown in Fig. 2(b). This behavior is in agreement with the superfluid-Mott transition for integer fillings.

In the regime where  $U \sim \Omega$ , the current becomes sensitive to changes of the  $U$  value and/or the number of particles, and a fast monotonic decaying of the current occurs as  $U$  grows [see Fig. 2(b)].

### B. Time-dependent system: local ac barrier

It has been theoretically and experimentally shown that the motion of particles in a lattice can be affected by the

action of an external ac field [19,20]. The periodic form of the ac driving satisfies the property  $\mathcal{A}(t) = \mathcal{A}(t + T)$  where  $T$  is the period. Since the frequency of the driving can be controlled on demand, different time scales of the system can be explored. These scales are characterized by the ratio between the frequency  $\omega$  of the driving and the characteristic tunneling rate  $\Omega$ . In particular, for the high frequency regime, i.e.,  $\omega/\Omega \gg 1$ , the time evolution of the system is governed by  $\Omega$  and can be separated from the characteristic time scale of the driving, i.e., the period  $T = 2\pi/\omega$ . Thus in this limiting case the time-periodic Hamiltonian,  $\hat{H}(t) = \hat{H}(t + T)$ , in the absence of interaction takes the effective form  $\hat{H}_{\text{eff}} = -\sum \Omega_{\text{eff}} (\hat{a}_i^\dagger \hat{a}_{i+1} + \hat{a}_{i+1}^\dagger \hat{a}_i)$ . Here  $\Omega_{\text{eff}} = \Omega J_0$  and  $J_0 = J_0(\frac{A}{\omega})$  is the Bessel function of the first kind and zero order, where  $A$  is the maximum of the ac-field amplitude for  $t \geq 0$ . Accordingly with this effective expression, the tunneling between nearest neighbors is reduced to zero when the  $A/\omega$  ratio takes the  $J_0$  root values [26]. In this case, the motion of bosonic particles in a lattice is interrupted and, therefore, the bosonic current of particles is halted. This process is usually referred to as either the dynamical localization [19] or the coherent destruction of tunneling [21,27].

With respect to the presence of the interaction term in the Hamiltonian system (1), it has been shown that this term in combination with an external ac field can induce a superfluid-Mott insulator transition in lattices [14]. Moreover, it has been observed that a time periodic modulation of the interaction term produces by itself a many-body coherent destruction of tunneling in lattices [28]. This has been exploited to generate exotic effective Hamiltonians [29] opening new avenues for further explorations.

## III. RESULTS

Despite the fact that the ac field acts only in one site of the ring lattice, the whole system becomes periodic in time, i.e., the Hamiltonian (1) is periodic in time. This implies that there exists a complete set of solutions,  $\psi_n(t)$ , of Eq. (1),

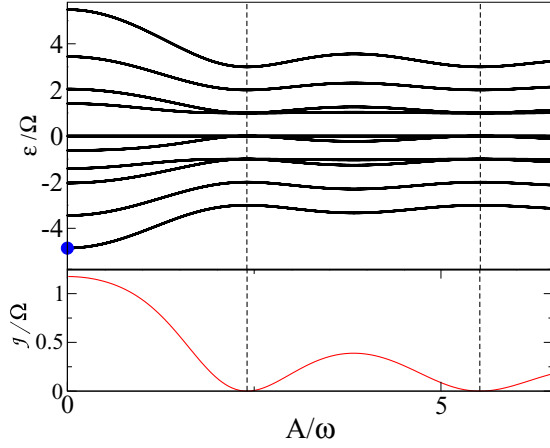


FIG. 3. (Color online) (Upper panel) Quasienergy spectrum vs amplitude  $A/\omega$ . The blue dot is the ground state depicted in Fig. 2(a) for  $U/\Omega = 0$ . (Lower panel) Bosonic current of the first quasienergy state plotted in the upper panel vs  $A/\omega$ . The parameters are  $\phi' = \pi/5$ ,  $U/\Omega = 0$ ,  $N = 3$  for  $L = 3$ .

usually referred to as Floquet states [30]. The Floquet states are periodic up to a phase, i.e.,  $\psi_n(t) = e^{-i\epsilon_n t/T} \Phi_n(t)$ , with  $\Phi_n(t+T) = \Phi_n(t)$ , where  $\epsilon_n \in [-\omega/2, \omega/2]$  are the so-called quasienergy values [31,32]. Here the Floquet states and their corresponding quasienergy values are computed using the same procedure proposed in Ref. [33].

The upper panel of Fig. 3 shows the quasienergy spectrum as a function of the  $A/\omega$  ratio, where the lowest band of the depicted bunch of quasienergy bands corresponds to the continuation of the ground state (unperturbed system) into the ac driving domain. When the  $A/\omega$  ratio is equal to the root values of the  $J_0$  Bessel function, several states of the ring lattice become degenerated, i.e., the quasienergy curves associated with these states cross each other at these root points. However, we observe that the two lowest quasienergy bands, depicted in Fig. 3, do not cross each other regardless of the maximum

amplitude value  $A$ . In order to distinguish these two bands from the other ones, in the following, we will refer to them as the first and second band, where the first one is the continuation of the ground state.

In the lower panel of Fig. 3, it is shown the magnitude  $\mathcal{J}$  vs the  $A/\omega$  ratio of the current of particles associated with the first and second quasienergy bands, plotted in the upper panel of Fig. 3. Notice that the current operator of particles  $\hat{\mathcal{J}}$  is defined in Eq. (2). In line with our previous analysis, the current, associated with the states of the first and second quasienergy bands vanishes when the  $A/\omega$  ratio is equal to the root values of the  $J_0$  Bessel function.

In the present work, we are interested in studying effects that arise in the Hamiltonian system (1) when the ac driving,  $\mathcal{A}(t)$ , is tailored so that the  $A/\omega$  ratio takes values in the vicinity of the roots of the  $J_0$  Bessel function.

In order to characterize the system, it is convenient to fix the  $A/\omega$  ratio in one root value of the  $J_0$  function and vary the  $U/\Omega$  parameter. In Fig. 4(a), we show the quasienergy spectrum as a function of the interaction  $U/\Omega$ . In this new parameter space, the first and second bands cross each other in a resonance point. We now impose the  $U/\Omega$  parameter to be at the resonance point in order to study the particle-current behavior of the first and second quasienergy bands. For that purpose, we let the  $A/\omega$  ratio vary around this point, as shown in Fig. 4(b). We observe that these currents change their sign as the  $A/\omega$  ratio takes values below and above the resonance point.

In order to systematically describe this phenomenology, let us consider the simplest case: two particles moving in a three-site ring. In the Fock basis the wave function of the system can be cast as

$$|\psi\rangle = a_1(t)|2,0,0\rangle + a_2(t)|1,1,0\rangle + a_3(t)|1,0,1\rangle + a_4(t)|0,2,0\rangle + a_5(t)|0,1,1\rangle + a_6(t)|0,0,2\rangle, \quad (3)$$

where  $|m_1, m_2, m_3\rangle$  denotes the state with occupancy number states  $m_\nu$  at the lattice sites  $\nu = 1, 2, 3$ . The  $a_\nu$  are complex

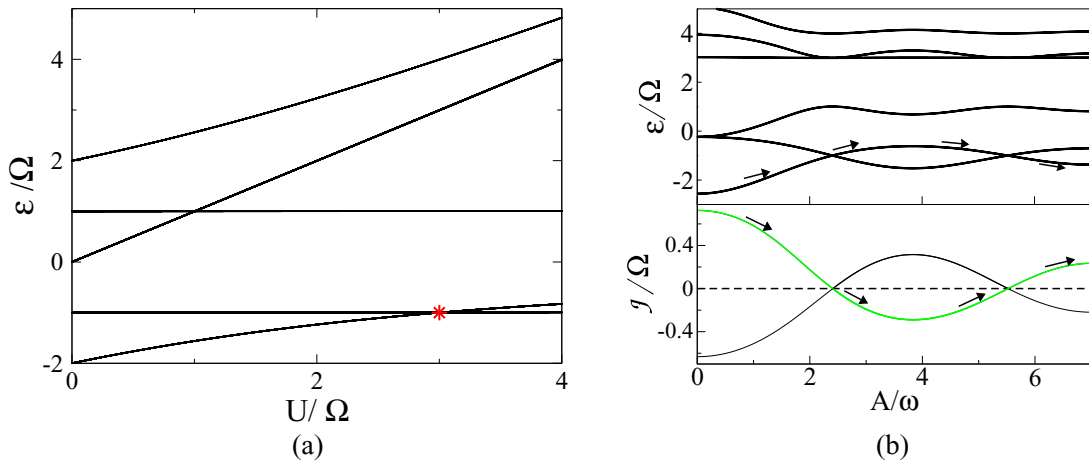


FIG. 4. (Color online) (a) Quasienergy  $\epsilon$  vs  $U/\Omega$ .  $A/\omega = 2.4048$ . (b) (Upper panel) Quasienergy vs  $A/\omega$ . The arrows indicate the continuation of the ground state into the ac driving domain (first quasienergy band). (Lower panel) Current of the first and second quasienergy states vs  $A/\omega$  for  $U = 3\Omega$ . The current for the first band is highlighted in green. Notice that in the crossings the current changes its sign. Two particles in three lattice sites.

coefficients which depend on time  $t$  and fulfill the normalization condition  $\sum_v |a_v|^2 = 1$ .

The evolution equations for the coefficients are

$$\begin{aligned}
 i\dot{a}_1 &= 2\mathcal{A}(t)a_1 + Ua_1 - \sqrt{2}\Omega a_2 e^{i\phi'} - \sqrt{2}\Omega a_3 e^{-i\phi'}, \\
 i\dot{a}_2 &= \mathcal{A}(t)a_2 - \sqrt{2}\Omega a_1 e^{-i\phi'} - \sqrt{2}\Omega a_4 e^{i\phi'} \\
 &\quad - \Omega a_3 e^{i\phi'} - \Omega a_5 e^{-i\phi'}, \\
 i\dot{a}_3 &= \mathcal{A}(t)a_3 - \Omega a_2 e^{-i\phi'} - \Omega a_5 e^{i\phi'} \\
 &\quad - \sqrt{2}\Omega a_6 e^{-i\phi'} - \sqrt{2}\Omega a_1 e^{i\phi'}, \\
 i\dot{a}_4 &= Ua_4 - \sqrt{2}\Omega a_2 e^{-i\phi'} - \sqrt{2}\Omega a_5 e^{i\phi'}, \\
 i\dot{a}_5 &= -\sqrt{2}\Omega a_4 e^{-i\phi'} - \Omega a_3 e^{-i\phi'} - \sqrt{2}\Omega a_6 e^{i\phi'} - \Omega a_2 e^{i\phi'}, \\
 i\dot{a}_6 &= -\sqrt{2}\Omega a_5 e^{-i\phi'} - \sqrt{2}\Omega a_3 e^{i\phi'} + Ua_6. \quad (4)
 \end{aligned}$$

Interestingly, the system (4) also can be made with two-dimensional photonic lattices, where the time  $t$  becomes the propagation coordinate of the system. In photonic systems the Peierls phases are created by periodically modulating parameters of coupled optical resonators or waveguides [34,35]. Likewise, ac fields can be mimicked by properly curving the waveguides [36].

In order to simplify the system (4) we introduce the transformation:  $a_1(t) = b_1(t)e^{-i\int_0^t 2\mathcal{A}(s)ds}$ ,  $a_2(t) = b_2(t)e^{-i\int_0^t \mathcal{A}(s)ds}$ ,  $a_3(t) = b_3(t)e^{-i\int_0^t \mathcal{A}(s)ds}$ ,  $a_4(t) = b_4$ ,  $a_5(t) = b_5(t)$ ,  $a_6(t) = b_6(t)$  [39]. Besides, we consider the dynamics at the high-frequency regime, where both the interaction and tunneling rate are much smaller than the frequency of the driving, i.e.,  $\{\Omega, U\} \ll \omega$  [37]. In the high-frequency regime the system (4) can be approached by [27]

$$\begin{aligned}
 i\dot{b}_1 &= Ub_1 - \sqrt{2}\Omega J_0(A/\omega)b_2 e^{i\phi'} - \sqrt{2}\Omega J_0(A/\omega)b_3 e^{-i\phi'}, \\
 i\dot{b}_2 &= -\sqrt{2}\Omega J_0(A/\omega)b_1 e^{-i\phi'} - \sqrt{2}\Omega J_0(A/\omega)b_4 e^{i\phi'} \\
 &\quad - \Omega b_3 e^{i\phi'} - \Omega J_0(A/\omega)b_5 e^{-i\phi'}, \\
 i\dot{b}_3 &= -\Omega b_2 e^{-i\phi'} - \Omega J_0(A/\omega)b_5 e^{i\phi'} - \sqrt{2}\Omega J_0(A/\omega)b_6 e^{-i\phi'} \\
 &\quad - \sqrt{2}\Omega J_0(A/\omega)b_1 e^{i\phi'}, \quad (5) \\
 i\dot{b}_4 &= Ub_4 - \sqrt{2}\Omega J_0(A/\omega)b_2 e^{-i\phi'} - \sqrt{2}\Omega b_5 e^{i\phi'}, \\
 i\dot{b}_5 &= -\sqrt{2}\Omega b_4 e^{-i\phi'} - \Omega J_0(A/\omega)b_3 e^{-i\phi'} - \sqrt{2}\Omega b_6 e^{i\phi'} \\
 &\quad - \Omega J_0(A/\omega)b_2 e^{i\phi'}, \\
 i\dot{b}_6 &= -\sqrt{2}\Omega b_5 e^{-i\phi'} - \sqrt{2}\Omega J_0(A/\omega)b_3 e^{i\phi'} + Ub_6,
 \end{aligned}$$

where  $A$  is the maximum amplitude of the  $\mathcal{A}(t)$  field and  $J_0(A/\omega)$  is the Bessel function of the first kind and zero order.

In order to get some insight into the dynamics of the system, let us consider the case when  $A/\omega$  rate equals one of the roots of the Bessel function, i.e.,  $A = A_0$  such that  $J_0(A_0/\omega) = 0$ . In this case, the system (5) reduces to

$$\begin{aligned}
 i\dot{b}_1 &= Ub_1, \\
 i\dot{b}_2 &= -\Omega b_3 e^{i\phi'}, \\
 i\dot{b}_3 &= -\Omega b_2 e^{-i\phi'}, \quad (6) \\
 i\dot{b}_4 &= Ub_4 - \sqrt{2}\Omega b_5 e^{i\phi'}, \\
 i\dot{b}_5 &= -\sqrt{2}\Omega b_4 e^{-i\phi'} - \sqrt{2}\Omega b_6 e^{i\phi'}, \\
 i\dot{b}_6 &= -\sqrt{2}\Omega b_5 e^{-i\phi'} + Ub_6.
 \end{aligned}$$

The system (6) can be written as  $i\dot{\mathbf{b}} = \mathbf{H}_0 \mathbf{b}$ , where the elements of the vector  $\mathbf{b}$  are the  $b_n$  functions. The matrix  $\mathbf{H}_0$  can be interpreted as an effective Hamiltonian. By using a Floquet ansatz of the form  $\mathbf{b}(t) = \mathbf{r} \exp(-iEt)$ , we obtain a stationary algebraic eigenvalue problem, where  $E$  is the multivalued eigenvalue. After solving this problem we obtain six eigenvalues, i.e.,  $E_0 = \frac{U - \sqrt{U^2 + 16\Omega^2}}{2}$ ,  $E_1 = -\Omega$ ,  $E_2 = U$ ,  $E_3 = U$ ,  $E_4 = \Omega$ , and  $E_5 = \frac{U + \sqrt{U^2 + 16\Omega^2}}{2}$ . These expressions, which are plotted vs the  $U$  parameter in Fig. 4(a), correspond to the quasienergy bands in the high-frequency regime. In particular, in the limiting case  $U = 0$ , we obtain  $E_0 = -2\Omega$ ,  $E_1 = -\Omega$ ,  $E_2 = 0$ ,  $E_3 = 0$ ,  $E_4 = \Omega$ , and  $E_5 = 2\Omega$ , where the  $E_0$  and  $E_1$  values correspond to the first and second quasienergy bands of the system (defined above), respectively. For our subsequent analysis, we focus on the resonant coupling between these two quasienergy bands.

The resonance point takes place at the intersection of the two bands and it is separated by a large gap from other quasienergy bands. Thus, the relevant physics of this system can be mainly attributed to the dynamics associated with these two bands.

As pointed out, for these two quasienergy bands, we can identify a resonance point, i.e., the point where  $E_0$  and  $E_1$  cross each other. This point corresponds to the values  $U = U_c = 3\Omega$  and  $E = E_c = -\Omega$ . [The resonance point is marked by a star in Fig. 4(a)].

Since the most important feature of these bands is their resonance point, to further analyze the system we impose the value  $U = U_c = 3\Omega$ . Under this consideration the two states, associated with the first and second quasienergy bands,  $E_0$  and  $E_1$ , read as  $\mathbf{r}^{(0)} = (0, 0, 0, \frac{e^{2i\phi'}}{\sqrt{10}}, \frac{2e^{i\phi'}}{\sqrt{5}}, \frac{1}{\sqrt{10}})$  and  $\mathbf{r}^{(1)} = (0, \frac{e^{i\phi'}}{\sqrt{2}}, \frac{1}{\sqrt{2}}, 0, 0, 0)$ , respectively. So, at the resonance point the initial wave function  $|\psi\rangle$ , defined in Eq. (3), can be written in the high-frequency regime as

$$\begin{aligned}
 |\psi_j^{(0)}\rangle &= r_1^{(j)}|2, 0, 0\rangle + r_2^{(j)}|1, 1, 0\rangle + r_3^{(j)}|1, 0, 1\rangle + r_4^{(j)}|0, 2, 0\rangle \\
 &\quad + r_5^{(j)}|0, 1, 1\rangle + r_6^{(j)}|0, 0, 2\rangle. \quad (7)
 \end{aligned}$$

In Eq. (7) the coefficients  $r_k^{(j)}$  are the elements of the vectors  $\mathbf{r}^{(j)}$  with  $j = 0, 1$  and  $k = 1, \dots, 6$ . These coefficients do not explicitly depend on the external driving, because the  $A/\omega$  ratio has been tailored to set to zero the  $J_0$  Bessel function. Moreover, the current of bosonic particles defined by Eq. (2) turns out to be zero exactly at the resonance point, because the matrix  $\mathbf{H}$ , derived from Eq. (6), consists of disconnected submatrices along the diagonal.

Now our main objective is to study the behavior of the current of the bosonic particles in the vicinity of this resonance point by using perturbation theory.

#### A. Perturbation theory of degenerated states: calculation of the current

Let us consider an amplitude of the form  $A = A_0 + \Delta$ , where  $J_0(A_0/\omega) = 0$  and  $\Delta$  is a small amplitude shift from the root value  $A_0$ . Since the current of particles vanishes only at the  $J_0$  root values, we expect a finite value of the particle current for a small amplitude shift  $\Delta$ . It is also important

to mention that in the vicinity of the  $A_0$  amplitude, the sign of the  $J_0$  Bessel function is governed by the  $\Delta$  shift, i.e.,  $J_0(A) = -\text{sign}(\Delta)|J_0(A)|$ .

The system (5) can be written as  $i\dot{\mathbf{b}} = \mathbf{H}\mathbf{b}$ , where the matrix  $\mathbf{H}$  is an effective Hamiltonian. This effective Hamiltonian can be written as  $\mathbf{H} = \mathbf{H}_0 + \mathbf{H}'$ , where  $\mathbf{H}_0$  corresponds to the effective Hamiltonian of the unperturbed system, given by Eq. (6), and  $\mathbf{H}' = \mathbf{H}'(A)$  is the perturbation term. The presence of a perturbation in the system introduces a gap between the first and the second bands, so an avoiding crossing appears. Since we are only interested in the bosonic particle dynamics in the vicinity of this avoiding crossing between the first and second bands, the effect of other quasienergy bands can be simply neglected. Notice that the effect of other quasienergy bands on the first and second bands are negligible due to the presence of a large bandgap. Therefore we are only concerned with the reduced system described by the states in Eq. (7).

Using the standard perturbation theory for degenerated eigenstates [40] we construct a matrix  $\mathbf{W}$  with elements  $w_{i,j} = \langle \psi_i^0 | \mathbf{H}' | \psi_j^0 \rangle$ . In the first-order correction, the eigenvalues of the reduced system are  $\tilde{E}_j = -\Omega + (-1)^j 3\sqrt{\frac{2}{5}}\Omega \cos(3\phi'/2)J_0(A)$  with  $j = 0, 1$ . Notice that these two energy bands depend not only on the absolute value of  $J_0(A')$  but also on its sign. With respect to the eigenvectors, at zero perturbation order they read as  $|\tilde{\psi}_j\rangle = \alpha_j|\psi_0^0\rangle + \beta_j|\psi_1^0\rangle$ , where  $(\alpha_j, \beta_j)$  with  $j = 0, 1$  are the components of the corresponding eigenvectors of  $\mathbf{W}$  [40]. The currents of bosonic particles associated with each of the bands can be estimated at zero-order perturbation theory by the expression  $\mathcal{J}_j = \langle \tilde{\psi}_j | \hat{\mathcal{J}} | \tilde{\psi}_j \rangle$  where the current operator  $\hat{\mathcal{J}}$  is defined by Eq. (2) and  $j = 0, 1$ . Thus an analytic estimation of the currents reads as

$$\mathcal{J}_j = \alpha_j \beta_j^* \langle \psi_1^0 | \hat{\mathcal{J}} | \psi_0^0 \rangle + \alpha_j^* \beta_j \langle \psi_0^0 | \hat{\mathcal{J}} | \psi_1^0 \rangle, \quad (8)$$

with  $j = 0, 1$ .

Substituting the values of  $|\psi_j^0\rangle$  from Eq. (7) into Eq. (8) yields

$$\mathcal{J}_j = (-1)^j \Omega \sqrt{\frac{2}{5}} \sin\left[\frac{3\phi'}{2}\right] \text{sgn}[\cos(\phi'/2)J_0(A')], \quad (9)$$

with  $j = 0, 1$ . This simply analytic result shows opposite signs of the current for the first and second bands in the vicinity of the amplitude  $A_0$ . In fact, in the vicinity of the degeneracy one can always, in good approximation, bring down the analysis of a multiple-band system to a two-band system, when a large band gap, with other bands, is present. In this scenario, one can show for a  $2 \times 2$  Hermitian matrix of the corresponding effective Hamiltonian that the wave functions are symmetric and antisymmetric (see e.g., [28]) and that the observables of the current appear in opposite signs. This implies that for a fixed Peierls phase  $\phi = L\phi' = 3\phi'$  the current of particles can be reversed depending on the  $\Delta$  sign. In other words, Eq. (9) shows that by controlling the amplitude  $A'$  of the external driving we can coherently reverse the current of particles in a ring lattice system. This nontrivial behavior is a very basic function expected to be present in atom circuits to perform operations for future quantum devices.

With respect to the generality of our analysis, it is important to remark that Eq. (9) follows from a reduced system, as mentioned above, so this result is independent of the Hilbert-space size. This means that similar resonance points occur for large number of particles and lattice sites, as we show below. In fact, in the high-frequency regime, we expect that the equation systems describing a larger number of particles and/or lattice sites will also depend on the  $J_0$  Bessel function, as we have shown in the system (5). Therefore, perturbation terms and effective Hamiltonians of these larger systems are also expected to depend on the  $J_0$  Bessel function. In particular, the first and second bands of these systems are also expected to have resonance points. So, the eigenvalues and eigenfunctions will also depend on the  $J_0$  Bessel function in these larger systems. This in turn means that particle currents associated with the crossing of the first and second quasienergy bands will behave similarly to that calculated in Eq. (9). Especially, we can expect reversion of the current of particles for larger systems.

## B. Lattice: numerical results

Here our interest is to show that, for systems with a larger number of particles and sites, the current of particles associated with first and second quasienergy bands indeed follows the qualitative behavior of the averaged system previously described. For example, in Fig. 5 we show the quasienergy spectrum as a function of  $U/\Omega$  for two cases, namely three particles in a four-lattice ring and five particles in a four-site lattice ring. We observe, as expected, that for a given  $U/\Omega$  value, the first and second quasienergy bands cross each other. Interestingly, in the cases analyzed in Fig. 5 we observe that in the vicinity of the crossing, the current of particles associated with the first quasienergy band exhibit values with opposite signs. This behavior is in line with our theoretical analysis leading to Eq. (9). It is important to remark that for a given  $U/\Omega$  value, if we extend the range of analysis of the  $A$  amplitude, we can observe a second crossing [see Fig. 4(b)], associated with the second root of the  $J_0$  Bessel function, which exhibits similar properties as the first one.

Our discussion, so far, has been based on the Floquet spectrum with strong emphasis in the quasienergy band associated with the ground state of the original unperturbed system. In fact, our ultimate goal is to reverse the current of the ground state of the undriven system. This is possible if the resonance point, described in the previous section, is reached. For this purpose, in the absence of the external driving, i.e.,  $A = 0$ , the ground state is initially prepared at the critical interaction amplitude  $U_c/\Omega$ . Afterwards, the amplitude  $A$  is turned up slowly making it possible to populate the quasienergy band. For convenience, we consider the amplitude  $A$  to change linearly in time, i.e.,  $A = \alpha t$ , where  $\alpha$  is the speed of change. In doing so, one can navigate through the energy spectrum, a process that can be controlled by properly changing the value of the speed  $\alpha$  [41]. This adiabatic following applies whenever the ramping speed is much smaller than the gap between the energy bands [42]. Besides, the relation  $\alpha/\omega \ll 1$  should be satisfied. Thus, following the quasienergy band the system passes through the resonance point and the current is reversed.

If the system is initially detuned from the critical value  $U_c/\Omega$  the degeneracy is lifted and a gap appears. If the energy

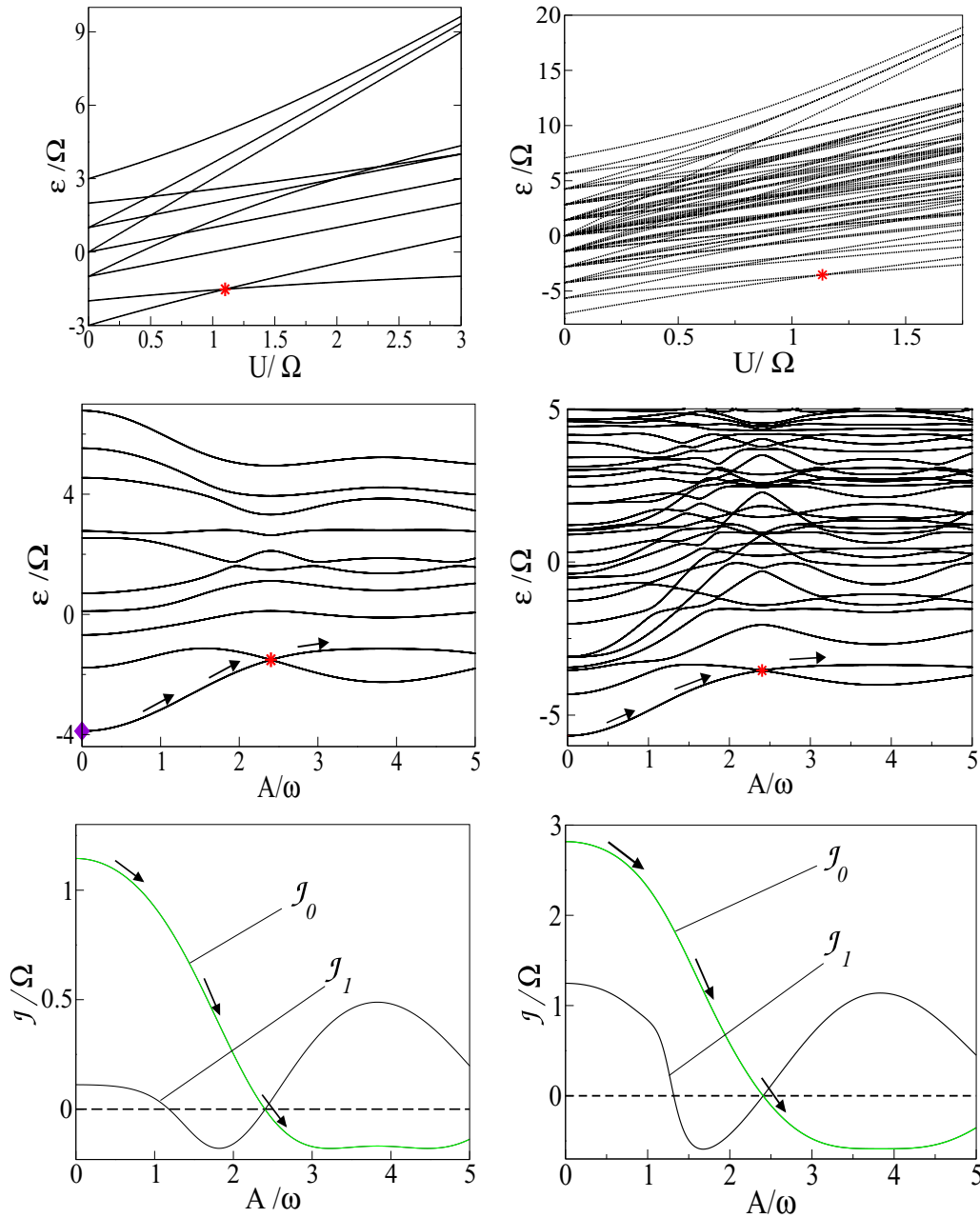


FIG. 5. (Color online) (Left panel) Three particles and three sites. (Right panel) Five particles and four sites. (First row) Quasienergy value vs interaction  $U/\Omega$  for  $A/\omega = 2.4048$ . (Second row) Quasienergy value vs amplitude of the driving  $A/\omega$ . (Left panel)  $U/\Omega = 1.105$ . The symbol of diamond corresponds to the ground state depicted in Fig. 2(a); (right panel)  $U/\Omega = 1.13$ . Stars depict the resonance point. (Third row) Current of the first quasienergy states vs amplitude of the driving  $A/\omega$ .  $\phi' = \pi/5$ . Dashed line indicates the zero current value.

splitting is very small, a jump from the first band to the second band occurs with a probability given by the Landau-Zener formula [43].

Figure 6 shows the current behavior after ramping  $A$  for various values of the interaction strength  $U/\Omega$ . The ramping is carried out from  $A = 0$  to  $A = A_{\max}$  with speed  $\alpha = 0.1$ . In a general scenario, after finishing the ramping process, the current ends up positive. Only in the near vicinity of  $U/\Omega = U_c/\Omega$ , the current becomes negative, as shown in Fig. 6(a).

This shows that reversing the current with ac fields is achievable by tuning the interaction and the amplitude of the

driving, setting a mechanism for the manipulation of persistent current of particles.

The fact that interaction between particles reverses the flux of particles, makes this mechanism sensitive to the number of particles. Figure 6 shows the dependence of  $U_c/\Omega$  as a function on the number of particles for three, four, and six lattice sites.  $U_c/\Omega$  dependence on the number of particles could eventually be used as a tool to estimate the number of particles that move across the lattice. Moreover, the dependence on the number of particles is interesting itself, since superfluid behavior could be modified when particles leave the matter wave.

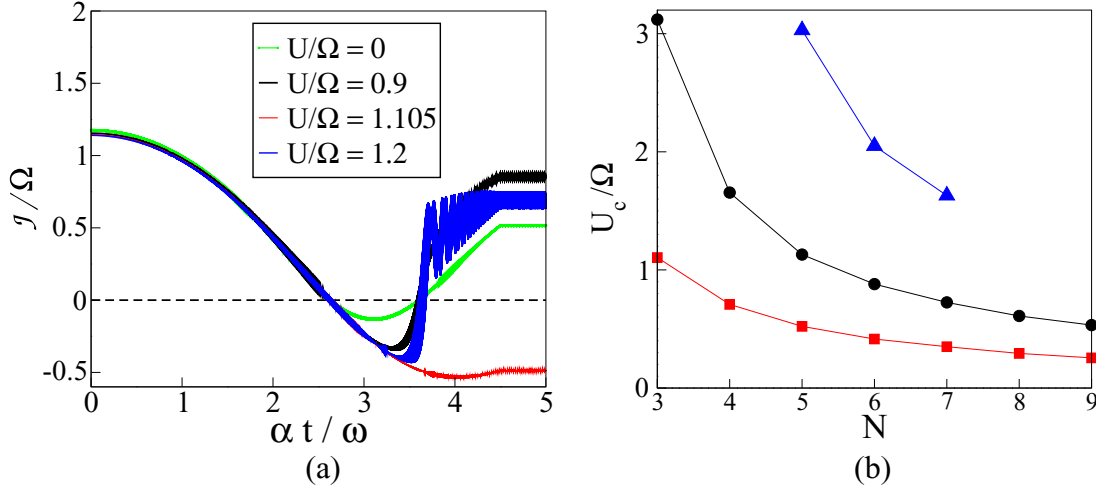


FIG. 6. (Color online) Current versus time where  $A = \alpha t$ . Ramping speed is  $\alpha = 0.1$ . (b) Critical interaction  $U_c/\Omega$  as a function of the number of particles  $N$  for rings with distinct lattice sites: squares, three sites; circles, four sites; up-triangles, six sites.  $\phi' = \pi/5$ .

#### IV. CONCLUSIONS

We have studied the behavior of currents of bosons moving in a ring lattice in the presence of an ac impurity. We have shown in a high-frequency regime that currents can be reversed by tuning the interaction between the particles. At some critical value of the interaction the ground state with a flux of particles moving in one direction resonantly interacts with an excited state of particles moving in the opposite direction. We first considered the simplest case of two particles and three lattice sites. In particular, we showed analytically the reversal behavior of the current for two bosons in three lattice sites and later extended their study numerically for more particles with three, four, and six lattice sites.

We also show the dependence of the critical interaction strength as a function of particles and lattice sites. This new mechanism can be used to coherently control these persistent currents in closed-loop atom circuits of future quantum devices. A particularly interesting implementation with

potential application of the present mechanism is in the read-out of quantum correlations between particles in ring lattices [44–46]. Moreover, the response of the system to an ac driving on a single site could also be of interest to recent experiments where the effects of introducing a barrier into the motion of matter waves in ring lattices have been investigated [3]. We have also pointed out the possibility of testing the dynamics of two particles in three lattice sites on a two-dimensional photonic lattice.

#### ACKNOWLEDGMENTS

This work was supported in part by the Fondo Nacional de Desarrollo Científico y Tecnológico (FONDECYT) Projects No. 1141223, No. 1130705, and No. 1150612, and by the Programa Iniciativa Científica Milenio (ICM) Grant No. 130001.

- 
- [1] R. Roth and K. Burnett, *Phys. Rev. A* **67**, 031602(R) (2003).  
 [2] L. Amico, A. Osterloh, and F. Cataliotti, *Phys. Rev. Lett.* **95**, 063201 (2005).  
 [3] A. Ramanathan *et al.*, *Phys. Rev. Lett.* **106**, 130401 (2011).  
 [4] M. Cominotti, D. Rossini, M. Rizzi, F. Hekking, and A. Minguzzi, *Phys. Rev. Lett.* **113**, 025301 (2014).  
 [5] S. Yu, P. Xu, M. Liu, X. He, J. Wang, and M. Zhan, *Phys. Rev. A* **90**, 062335 (2014).  
 [6] C. Ryu, P. W. Blackburn, A. A. Blinova, and M. G. Boshier, *Phys. Rev. Lett.* **111**, 205301 (2013).  
 [7] M. Lewenstein, A. Sanpera, V. Ahufinger, B. Damski, A. Sen, and U. Sen, *Adv. Phys.* **56**, 243 (2007).  
 [8] I. Bloch, J. Dalibard, and W. Zwerger, *Rev. Mod. Phys.* **80**, 885 (2008).  
 [9] M. Greiner, O. Mandel, T. Esslinger, Th. W. Hänsch, and I. Bloch, *Nature (London)* **415**, 39 (2002).  
 [10] O. Morsch and M. Oberthaler, *Rev. Mod. Phys.* **78**, 179 (2006).  
 [11] D. Jaksch and P. Zoller, *New J. Phys.* **5**, 56 (2003); J. Dalibard, F. Gerbier, G. Juzeliunas, and P. Öhberg, *Rev. Mod. Phys.* **83**, 1523 (2011); M. Aidelsburger, M. Atala, S. Nascimbène, S. Trotzky, Y.-A. Chen, and I. Bloch, *Phys. Rev. Lett.* **107**, 255301 (2011); N. Goldman, A. Kubasiak, A. Bermudez, P. Gaspard, M. Lewenstein, and M. A. Martin-Delgado, *ibid.* **103**, 035301 (2009); K. Jiménez-García, L. J. LeBlanc, R. A. Williams, M. C. Beeler, A. R. Perry, and I. B. Spielman, *ibid.* **108**, 225303 (2012); J. Struck, C. Ölschläger, M. Weinberg, P. Hauke, J. Simonet, A. Eckardt, M. Lewenstein, K. Sengstock, and P. Windpassinger, *ibid.* **108**, 225304 (2012).



- [12] G. Bouzerar, D. Poilblanc, and G. Montambaux, *Phys. Rev. B* **49**, 8258 (1994).
- [13] A. Eckardt, Ch. Weiss, and M. Holthaus, *Phys. Rev. Lett.* **95**, 260404 (2005).
- [14] H. Lignier, C. Sias, D. Ciampini, Y. Singh, A. Zenesini, O. Morsch, and E. Arimondo, *Phys. Rev. Lett.* **99**, 220403 (2007).
- [15] B. Wu nad Q. Niu, *Phys. Rev. A* **61**, 023402 (2000).
- [16] L. Morales-Molina and S. Flach, *New. J. Phys.* **10**, 013008 (2008).
- [17] L. Morales-Molina and E. Arevalo, *Phys. Rev. A* **82**, 013642 (2010).
- [18] S. Inouye *et al.*, *Nature (London)* **392**, 151 (1998); A. Dirks, K. Mikelsons, J. K. Freericks, and H. R. Krishnamurthy, [arXiv:1408.0206](https://arxiv.org/abs/1408.0206).
- [19] D. H. Dunlap and V. M. Kenkre, *Phys. Rev. B* **34**, 3625 (1986).
- [20] E. Kierig, U. Schnorrberger, A. Schietinger, J. Tomkovic, and M. K. Oberthaler, *Phys. Rev. Lett.* **100**, 190405 (2008).
- [21] F. Grossmann, T. Dittrich, P. Jung, and P. Hänggi, *Phys. Rev. Lett.* **67**, 516 (1991).
- [22] T. Salger, C. Geckeler, S. Kling, and M. Weitz, *Phys. Rev. Lett.* **99**, 190405 (2007).
- [23] T. Salger *et al.*, *Science* **326**, 1241 (2009).
- [24] S. Fölling *et al.*, *Nature (London)* **448**, 1029 (2007).
- [25] P. Windpassinger and K. Sengstock, *Rep. Prog. Phys.* **76**, 086401 (2013).
- [26] M. Abramowitz and I. A. Stegun, *Handbook of Mathematical Functions* (NIST, Gaithersburg, 1972).
- [27] Y. Kayanuma and K. Saito, *Phys. Rev. A* **77**, 010101 (2008).
- [28] J. Gong, L. Morales-Molina, and P. Hänggi, *Phys. Rev. Lett.* **103**, 133002 (2009).
- [29] A. Rapp, X. Deng, and L. Santos, *Phys. Rev. Lett.* **109**, 203005 (2012); S. Greschner, G. Sun, D. Poletti, and L. Santos, *ibid.* **113**, 215303 (2014); S. Greschner, L. Santos, and D. Poletti, *ibid.* **113**, 183002 (2014).
- [30] M. Grifoni and P. Hänggi, *Phys. Rep.* **304**, 229 (1998).
- [31] J. H. Shirley, *Phys. Rev.* **138**, B979 (1965).
- [32] H. Sambe, *Phys. Rev. A* **7**, 2203 (1973).
- [33] S. Denisov, L. Morales-Molina, and S. Flach, *Europhys. Lett.* **79**, 10007 (2007); S. Denisov, L. Morales-Molina, S. Flach, and P. Hänggi, *Phys. Rev. A* **75**, 063424 (2007).
- [34] S. Longhi, *Opt. Lett.* **38**, 3570 (2013).
- [35] K. Fang, Z. Yu, and Sh. Fan, *Nature Photon.* **6**, 782 (2012).
- [36] G. Della Valle, M. Ornigotti, E. Cianci, V. Foglietti, P. Laporta, and S. Longhi, *Phys. Rev. Lett.* **98**, 263601 (2007).
- [37] In the regime where the interaction strength is of the same order of magnitude of the driving frequency, additional terms appear in the effective Hamiltonian as shown in [38].
- [38] A. Verdeny, A. Mielke, and F. Mintert, *Phys. Rev. Lett.* **111**, 175301 (2013).
- [39] G. Lu, L.-B. Fu, J. Liu, and W. Hai, *Phys. Rev. A* **89**, 033428 (2014).
- [40] C. Cohen-Tannoudji, B. Diu, and F. Lalaoë, *Quantum Mechanics*, Vol. II (John Wiley & Sons, New York, 1977).
- [41] G. E. Murgida, D. A. Wisniacki, and P. I. Tamborenea, *Phys. Rev. Lett.* **99**, 036806 (2007); L. Morales-Molina, S. Flach, and J. B. Gong, *Europhys. Lett.* **83**, 40005 (2008); E. Arevalo and L. Morales-Molina, *ibid.* **96**, 60011 (2011).
- [42] D. M. Tong, K. Singh, L. C. Kwek, and C. H. Oh, *Phys. Rev. Lett.* **95**, 110407 (2005).
- [43] L. D. Landau, *Phys. Z. Sowjetunion* **2**, 46 (1932); C. Zener, *Proc. R. Soc. London, Ser. A* **137**, 696 (1932).
- [44] L. Morales-Molina, S. A. Reyes, and M. Orszag, *Phys. Rev. A* **86**, 033629 (2012).
- [45] S. A. Reyes, L. Morales-Molina, M. Orszag, and D. Spenher, *Europhys. Lett.* **108**, 20010 (2014).
- [46] L. Amico, D. Aghamalyan, H. Crepaz, F. Auksztol, R. Dumke, and L.-C. Kwek, *Sci. Rep.* **4**, 4298 (2014).